Received: 20 July 2025 | Revised: 8 September 2025 | Accepted: 25 September 2025 | Published online: 14 October 2025

RESEARCH ARTICLE

Smart Wearable Technology
2025, Vol. 00(00) 1–9
DOI: 10.47852/bonviewSWT52026869

BON VIEW PUBLISHING

From Wires to Wearables (1): Clinical equivalence with an Axis-Aware Validation of a Wearable ECG System (Sydäntek) with Compressed Lead Geometry

Sugandhi Gopal[1,*], Prabhavathi Bhat[2], Sharada Sivaram[3], V. J. Karthikeyan[4], Mukund Prabhu[5], Mohith Subramanian[6], Vishwa Teja Reddy[6] and Aishwarya Srinivasan[7]

[1]*Interventional Cardiologist, Founder Director, Carditek Medical Devices, India*

[2]*Sri Jayadeva Institute of Cardiovascular Sciences & Research, India*

[3]*Saveetha Medical College, India*

[4]*The University of Manchester, UK*

[5]*Manipal Academy for Higher Education, India*

[6]*Carditek Medical Devices, India*

[7]*BMS College of Engineering, Bengaluru, India*

Abstract: Conventional 12-lead electrocardiogram (ECG) systems, reliant on wired configurations and distal limb electrodes, restrict patient mobility and hinder continuous monitoring. Recent advances in wearable ECG aim to deliver diagnostic-grade fidelity in ambulatory settings. Sydäntek—a compact wearable ECG developed by Carditek Medical Devices—addresses these limitations by compressing Einthoven's triangle into a 5 × 5 cm patch positioned at the left shoulder crease. This novel geometry enables full 12-lead acquisition without compromising signal fidelity. In a clinical comparison with a standard ECG system (Welch Allyn CardioPerfect™), Sydäntek's performance was evaluated using Bland–Altman analysis and polar histogram visualization across a stratified population. Patients were grouped by baseline QRS axis into three ranges (−30° to 0°, 0° to +45°, and +45° to +90°) to assess axis-dependent variability. Sydäntek demonstrated consistent waveform morphology and a predictable QRS axis rotation (∼ +14°), attributable to anterior repositioning of limb leads. Polar histograms revealed a leftward skew without significant outliers. Subgroup Bland–Altman analysis showed systematic, baseline-dependent variability: the 0° to +45° group exhibited the narrowest limits of agreement, while the −30° to 0° cohort displayed greater dispersion. Applying a +14° correction effectively minimized axis bias within the clinically relevant −30° to +90° range, preserving diagnostic waveform integrity. Overall, Sydäntek achieves clinical equivalence with standard ECG through a geometry-driven axis adaptation that is consistent, manageable, and clinically acceptable. Its compact, wire-free form factor enables high-fidelity cardiac monitoring in real-time ambulatory settings—demonstrating that spatial innovation can coexist with gold-standard diagnostics and advance the ECG into wearable practice.

Keywords: wearable 12-lead ECG, QRS axis correction, Bland–Altman analysis, electrode geometry, clinical equivalence

1. Graphical Abstract Summary

This multi-panel figure illustrates Sydäntek's core innovation: the spatial compression of Einthoven's triangle into a compact 5 × 5 cm patch positioned at the left upper shoulder crease. By reconfiguring lead geometry within this wearable form factor, Sydäntek enables real-time, untethered 12-lead electrocardiogram (ECG) acquisition without compromising diagnostic fidelity or interpretive confidence.

The figure contrasts classical and wearable ECG systems, highlighting Sydäntek's anterior lead repositioning and the resulting ∼ +14° rotation in frontal axis interpretation. Despite this predictable geometric shift, waveform morphology and vector symmetry are preserved. Coronary territory mapping, axis histograms, and polar plots confirm that spatial compression does not degrade clinical utility. Instead, Sydäntek adapts gold-standard ECG principles to modern wearable constraints—delivering high-fidelity cardiac monitoring in a wire-free, ambulatory format.

2. Introduction

2.1. Legacy of the 12-lead ECG

The 12-lead ECG remains a cornerstone in the evaluation of cardiac rhythm, ischemia, and conduction abnormalities. Despite technological advances, its foundational geometry is still based on

*Corresponding author: Sugandhi Gopal, Interventional Cardiologist, Founder Director, Carditek Medical Devices, India. Email: sugopal@carditek.com

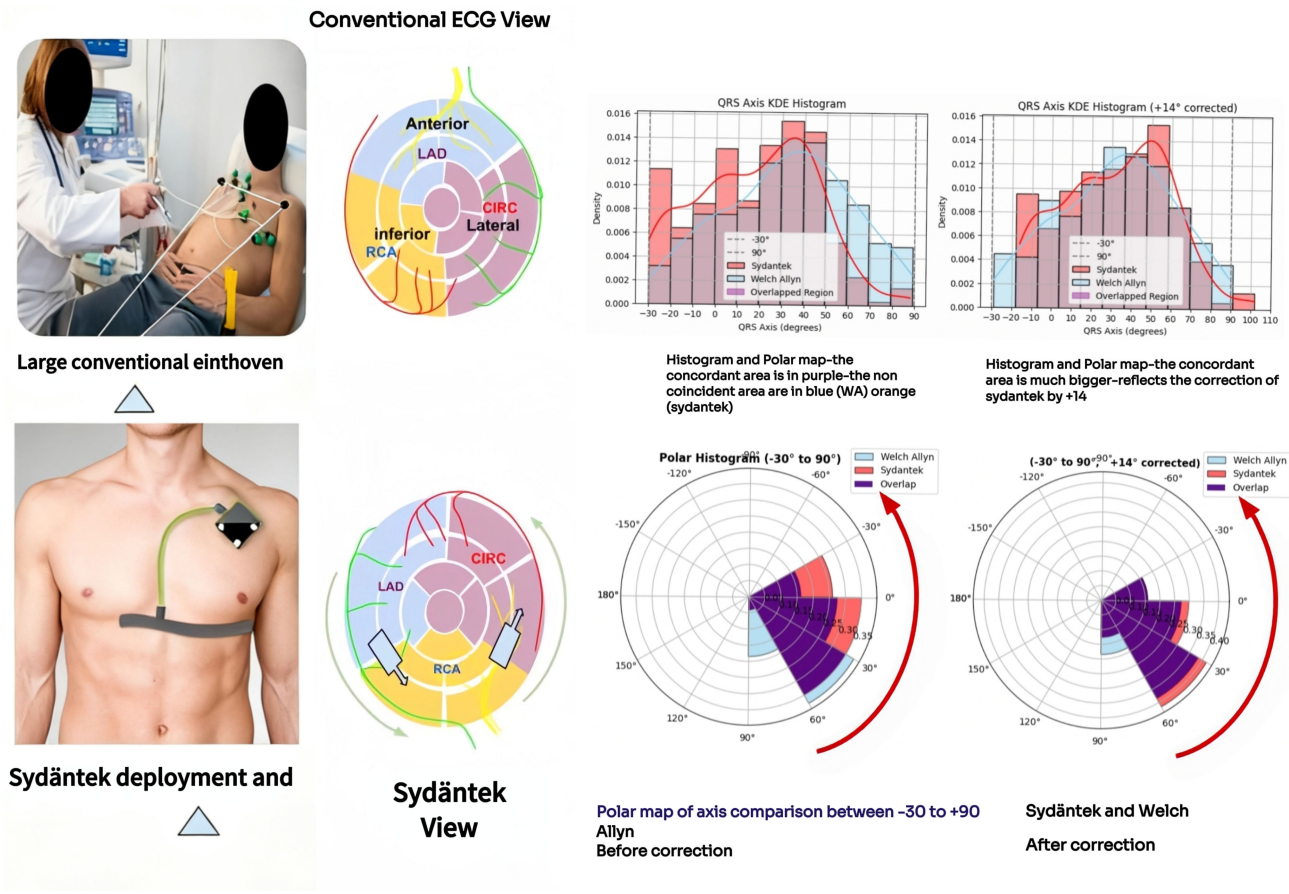

Einthoven's triangle—a spatial construct placing electrodes on the right arm, left arm, and left leg. These distal placements define the orientation of limb leads I, II, and III, projecting electrical activity across the frontal plane and informing clinical interpretation for decades [1–3].

2.2. Limitations of traditional geometry

This arrangement was designed in an era of wired systems, rudimentary amplification, and immobile patients. Today's clinical landscape emphasizes compactness, mobility, and continuity of care. Advances in capacitive sensors, microelectronics, and wireless communication now enable full 12-lead ECG acquisition in portable, untethered systems. These innovations challenge traditional geometry—particularly when limb leads are repositioned to proximal thoracic sites [4, 5].

2.3. Sydäntek: A modern reinterpretation

Sydäntek, a wearable ECG device developed by Carditek Medical Devices, embodies this evolution. It uses a 5 × 5 cm capacitive patch for limb leads placed at the left shoulder crease and a precordial chest strip for V1–V6 capture. With Bluetooth Low Energy (BLE) transmission and encrypted cloud storage (Pulse Vault™), the system enables high-resolution, real-time ECG monitoring (286 nV resolution) without sacrificing diagnostic channels. This compressed configuration effectively reorients Einthoven's triangle over the upper anterior chest, enabling wire-free 12-lead acquisition in ambulatory settings.

2.4. Axis rotation and clinical interpretability

A predictable consequence of this lead redesign is frontal plane QRS axis rotation, primarily due to superior repositioning of the left leg electrode. While early modeling suggested a ~25° shift, Bland–Altman analysis localized the effective offset to +14° within the clinically relevant axis window (−30° to +90°). This realignment subtly redistributes electrical territories—particularly in inferior and lateral leads—without disrupting diagnostic quadrant placement. Prior vectorcardiographic studies support the notion that such reorientations preserve clinical interpretability when vector trajectories remain coherent [6, 7].

2.5. Axis in clinical context

Axis is rarely interpreted in isolation. While relevant in diagnosing fascicular blocks, ventricular hypertrophy, or specific arrhythmias, it plays a supportive role compared to waveform morphology and temporal intervals. A consistent and correctable offset—if not disruptive to waveform integrity—can be readily accommodated in clinical workflows.

2.6. Study objective and hypothesis

This study evaluates the clinical equivalence of Sydäntek compared to a standard ECG system in terms of waveform fidelity and axis interpretation. By stratifying patients into baseline axis subgroups and applying visual and statistical overlay methods, we aim to demonstrate that wearable redesign can preserve diagnostic utility.

We hypothesize that Sydäntek's proximal lead geometry enables clinically interpretable axis measurements and waveform fidelity comparable to standard 12-lead ECG systems.

2.7. Transparency and certification considerations

A primary challenge in life-critical real-time systems lies in designing bug-free medical device software. Implantable devices

have been extensively studied, with firmware recalls on the rise. To maintain transparency, we chose not to correct the axis shift algorithmically but instead declared the offset explicitly. This approach supports seamless integration into clinical workflows and may expedite medical device certification [8].

3. Materials and Methods

3.1. Device configuration and axis interpretation framework

Electrocardiographic signals were recorded using Sydäntek, a wearable ECG device developed by Carditek Medical Devices. It uses a 5 × 5 cm capacitive patch for limb leads at the left shoulder crease and a lateral chest strip for V1–V6. Signals stream in real time via BLE, with encrypted storage managed by Pulse Vault™. The system supports high-resolution acquisition (286 nV), suitable for diagnostic 12-lead ECGs and ambulatory Holter monitoring. Signal quality and resistance to motion artifacts were validated per wearable ECG benchmarking guidelines [7].

Because the limb leads are placed on the upper chest, their geometry differs from the classic Einthoven triangle. This reorientation causes predictable changes in the QRS axis, mainly due to elevation of the left leg vector. Axis metrics—including QRS, P-wave, and T-wave angles—were calculated using frontal plane projections [9], and coupling angles were measured using large cohort methods from recent studies by Kayyali et al. [1]. These metrics guided patient stratification.

Annotations were entered via a JSON-linked digital sheet, capturing waveform quality, axis data, and stratification flags. Longitudinal tracking used temporal drift fields to monitor anatomical or electrical changes. Additional imaging metrics, like the sphericity index, helped interpret axis shifts [10].

Validation methods included waveform overlays, Bland–Altman plots, and quadrant integrity tests to confirm vector consistency between wearable and standard ECG systems [6, 11]. The framework aligns with modern ECG algorithms that encode axis features as latent vectors in deep-learning models [2, 3].

Following ISO/IEC 80601-2-86, no software correction was applied to axis deviations. Instead, offsets were measured and reported transparently to support clinical traceability and regulatory standards [3, 4]. This approach also reduces risks from firmware instability—a growing concern in life-critical embedded systems [12].

The dataset reflects a cardiac-enriched population, as 343 patients were recruited from a tertiary cardiac hospital and 49 from a wellness clinic. While this skews prevalence toward pathology, it enhances the robustness of axis stratification and waveform stress-testing under real-world clinical conditions. The inclusion of wellness clinic data provides a comparative baseline for "normative axis distribution."

Figure 1 illustrates the evolution of ECG monitoring platforms, culminating in the Sydäntek wearable solution. Figure 1(a) Conventional 12-Lead ECG: Standard clinical setup involving multiple wired electrodes placed on the limbs and chest. The patient is supine and tethered to a bedside system, underscoring the spatial and mobility constraints of traditional ECG acquisition. Figure 1(b) Two-Lead Short-Term Patch (Lead I–II, 30-Second Capture): Common ambulatory patch solution used for brief rhythm screening. While compact, it offers limited spatial resolution and lacks full 12-lead diagnostic capability. Figure 1(c) Sydäntek 12-Lead Wearable ECG System: Innovative configuration using a 5 × 5 cm capacitive patch at the left shoulder crease for limb leads, coupled with a short lateral strip for precordial leads. This setup enables untethered, high-fidelity 12-lead ECG acquisition with real-time wireless transmission and cloud-based storage—compressing conventional geometry into a compact form factor without loss of diagnostic integrity. Interpretive Insight: This figure introduces Sydäntek's clinical promise: preserving full-lead fidelity within a wearable architecture, overcoming legacy wiring constraints while maintaining interpretive parity with standard ECG systems.

Figure 1
Comparative configurations of conventional and wearable ECG systems—used for illustrative purpose only to show deployment

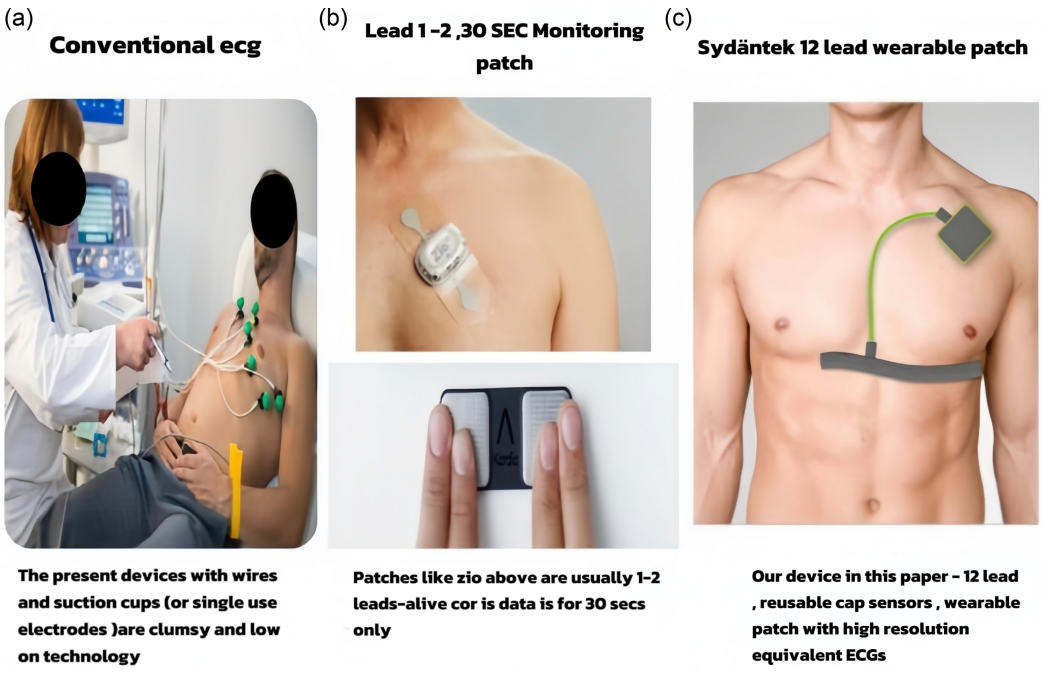

3.2. Comparator and validation workflow

Comparator system: The reference ECG system used was Welch Allyn CardioPerfect™, a clinically validated 12-lead platform. All recordings were acquired under resting conditions with standard electrode placement.

Patient stratification: Participants were grouped based on baseline QRS axis into three clinically defined bins:
Left axis deviation (LAD) (< −30°)
Normal axis (−30° to +90°)
Right axis deviation (RAD) (> +90°): This stratification enabled axis-dependent analysis of waveform agreement.

Data acquisition protocol: Sydäntek and comparator recordings were obtained sequentially within a 5-minute window to minimize physiological drift. Electrode placement for Sydäntek followed its proprietary shoulder-crease configuration.

Signal processing: All Sydäntek signals underwent embedded preprocessing, including proprietary noise-handling algorithms and Butterworth filtering. Only recordings passing internal quality thresholds were included in the analysis.

Agreement analysis: Bland–Altman plots and polar histograms were used to assess waveform and axis agreement. Subgroup analysis was performed across axis bins to evaluate systematic variability. Residual axis error distributions and quadrant misclassification rates were quantified pre- and post-correction.

4. Results

4.1. QRS axis measurement and cohort stratification

Frontal plane QRS axis data were extracted from 392 patients who underwent paired ECG acquisition using Sydäntek and a standard 12-lead system (Welch Allyn). Of these, 347 patients were classified as having a normal axis (−30° to +90°) and formed the basis for distribution and correction analysis. Cross-validation confirmed consistent directional trends between both systems.

4.2. Axis distribution, offset, and quadrant fidelity

Thirty-eight patients showed LAD (< −30°), and seven had RAD (> +90°). Across all groups, Sydäntek preserved diagnostic quadrant fidelity—mapping vectors to equivalent sectors despite geometric lead repositioning. Realignment in the RAD group remained within clinically acceptable limits, consistent with known redistribution patterns when limb electrodes are placed proximally [4, 11].

Sydäntek's compact lead geometry induced a consistent frontal plane axis rotation. Initial modeling suggested a ∼25° leftward shift, but Bland–Altman analysis localized the mean offset to +14°, well within the clinical window. This angular change reflects spatial transformation rather than signal distortion, validating the fidelity of Sydäntek's configuration.

4.3. Visual distribution and correctional impact

Axis values were binned in 15° increments from −90° to +120° and plotted using Python (matplotlib) to assess clustering. The dominant distribution fell between −30° and +45°, with Sydäntek values showing a mild leftward skew. Polar density plots confirmed quadrant preservation with no dispersion into diagnostically ambiguous zones.

Values beyond ±90° were flagged as extreme axis cases. No recordings exceeded +120° or dropped below −90°, and all remained within interpretable clinical ranges.

To assess correctional impact, the Bland–Altman analysis was applied across the normal axis range. A +14° adjustment minimized systematic bias and eliminated quadrant misclassification. Kernel density overlays and polar histograms demonstrated directional realignment and vector clustering post-correction, confirming that the offset was geometry-driven—not signal-inherent.

Figure 2(a): Raw Comparison: Bland–Altman plot comparing uncorrected QRS axis values between Welch Allyn and Sydäntek ($n = 347$). The plot shows a systematic bias and asymmetrical limits of agreement, indicating a consistent angular offset from wearable lead geometry. Figure 2(b) After +14° Correction: Same analysis following empirical +14° correction applied to Sydäntek data. The bias line centers near zero, with improved symmetry and narrower limits—supporting the +14° adjustment as optimal for harmonizing axis interpretation across systems. Based on our trial of corrections of the bias line (in the Bland–Altman analysis graphs*), we were able to identify an optimization of +14° as the axis correction to reach a systematic bias of 0° and preserve quadrant integrity. This helped us further validate Sydäntek's clinical equivalence mathematically.

*Bland–Altman analysis is widely used in medical research to assess agreement between two measurement methods by quantifying bias and limits of agreement. In this study, it enabled empirical

Figure 2

Bland–Altman plots of QRS axis agreement before and after +14° correction. (a) Raw comparison: Bland–Altman plot comparing uncorrected QRS axis values between Welch Allyn and Sydäntek (n = 347) and (b) after +14° correction: same analysis following empirical +14° correction applied to Sydäntek data

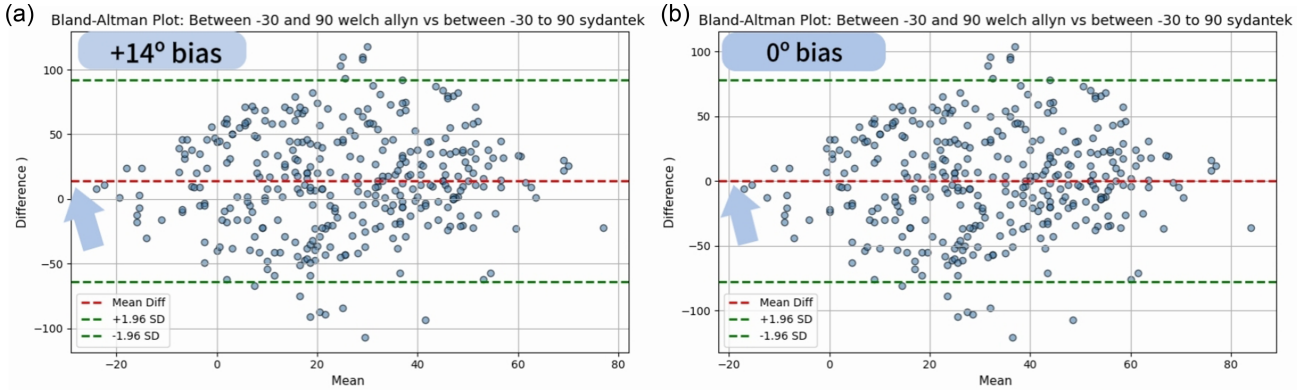

identification of a +14° correction that minimized systematic axis deviation between Sydäntek and Welch Allyn—validating the wearable system's diagnostic equivalence through direct inter-method comparison.

4.4. Clinical compatibility and subgroup agreement

Since axis metrics are interpreted alongside waveform morphology, rhythm, and intervals, the geometric shift was evaluated for diagnostic impact. All observed offsets remained within interpretable limits and did not compromise waveform integrity. This supports compatibility with clinical workflows and aligns with findings from cardiac digital twin-based axis coupling research by Qian et al. [5] and UK Biobank studies by Ugurlu et al. [6].

Subgroup Bland–Altman analysis within the normal axis range showed:

1) 0° to +45°: Narrowest agreement limits and minimal bias
2) +45° to +90°: Slightly wider intervals, but consistent directional fidelity
3) −30° to 0°: Broadest spread due to proximity to anatomical transition zones; no quadrant misalignment occurred

Even in LAD and RAD subgroups, Sydäntek maintained quadrant alignment. These trends mirror anatomical–electrical discrepancies documented in multimodal cohort analyses [6] and reinforce the device's diagnostic reliability.

5. Discussion

5.1. Axis behavior and fidelity across subgroups

This study confirms that Sydäntek introduces a consistent leftward QRS axis rotation across normal and abnormal cohorts, attributed to wearable-specific lead geometry. When corrected by +14°, the displacement preserves quadrant alignment and supports clinical equivalence with conventional interpretation. These findings echo prior vectorcardiographic work emphasizing angular coherence over absolute values [13, 14]. The observed realignment falls within anatomical–electrical coupling variability documented in large cohort studies like UK Biobank [1, 8] and CT-based models [3]. While wearable validation literature has focused on rhythm and interval fidelity [15, 16], axis consistency remains underexplored—this study helps bridge that gap.

Histogram overlays, kernel density estimation (KDE), and polar plots showed spatially consistent and reversible axis divergence. Even in marked LAD or RAD cases, Sydäntek maintained quadrant integrity, reinforcing robustness across diverse anatomies.

Performed all analyses in Google Colab (Python 3.12.11) using default versions of pandas, numpy, and matplotlib. Histograms used a 10° bin width with Gaussian KDE, normalized to unit area. Polar histograms covered with 30° bins, normalized per device, plotted on a polar axis (θ=0° rightward, clockwise increase). No custom smoothing beyond the specified KDE was applied.

Figure 3 illustrates the comparative analysis, correction, and clinical equivalence of Sydäntek's wearable ECG system, assessed using two types of histograms and two patient groups: those with normal axis and those with extreme axis deviation. A consistent +14° correction harmonizes Sydäntek's axis readings with conventional limb-lead geometry across all strata, preserving quadrant interpretation and supporting diagnostic fidelity. Figure 3(a) Raw Data (Pre-Correction): (a1) Histogram of uncorrected QRS axis values from Welch Allyn (blue) and Sydäntek (pink), across 347 patients. Sydäntek shows a systematic leftward shift, consistent with anterior lead repositioning inherent to its wearable form factor. (a2) Polar density map for the normal axis group: Sydäntek vectors (black) exhibit angular displacement relative to Welch Allyn (gray) and yet maintain quadrant alignment—indicating preserved interpretive structure despite geometric shift. (a3) Polar map for the left and right axis deviation group: Sydäntek vectors remain confined within the diagnostic quadrant, confirming axis fidelity even under spatial compression. Figure 3(b) Post-Correction (+14° Applied): (b1) Histogram overlay after correction: Sydäntek axis values realign centrally with Welch Allyn, resolving systematic bias and narrowing distribution spread. (b2) Polar plot for corrected normal axis group: Adjusted Sydäntek vectors (red) converge with conventional vectors (gray), validating the geometric correction and restoring interpretive concordance. (b3) Polar plot for corrected left and right axis deviation group: Vectors realign to appropriate clinical zones, confirming that observed discrepancies were geometric rather than pathological. Conclusion: When corrected for its predictable +14° axis rotation, Sydantek achieves near-complete concordance with conventional ECG geometry. This confirms that spatial innovation can coexist with diagnostic rigor—enabling medical rigor from a wearable device.

5.2. Clinical compatibility and interpretive confidence

These results align with interpretive frameworks that prioritize waveform morphology, timing, and rhythm over precise axis values [2, 17]. Axis is contextual—critical in fascicular blocks or hypertrophy, but often adjunctive to QRS changes. Accordingly, the ∼14° angular shift, with preserved waveform fidelity, is clinically negligible and easily accommodated.

Sydäntek's physiological design and validated geometry demonstrate that wearable systems can match the interpretive reliability of traditional platforms. By preserving electrode semantics and waveform structure—even with compressed architecture—it enables ambulatory, high-resolution cardiac monitoring without loss of diagnostic integrity [4, 10].

5.3. Territory recalibration and spatial adaptation

The axis shift invites a reframing of spatial expectations, especially for clinicians accustomed to traditional limb-lead orientation. Superior repositioning of the left leg electrode compresses Einthoven's triangle, subtly shifting projections of inferior and lateral activity.

Classical inferior vectors (leads II, III) may redistribute toward V5–V6, while anterior forces may express more in III and aVF. This reflects a change in viewing angle—not signal degradation—as reinforced in morphologic transformation studies and pediatric/post-surgical ECG interpretations.

Importantly, the adjustment is cognitively intuitive. Once the ∼14° offset is understood, interpretation becomes a matter of spatial awareness rather than retraining.

Figure 3
Comparative axis distribution, correction, and equivalence between Sydäntek and conventional ECG

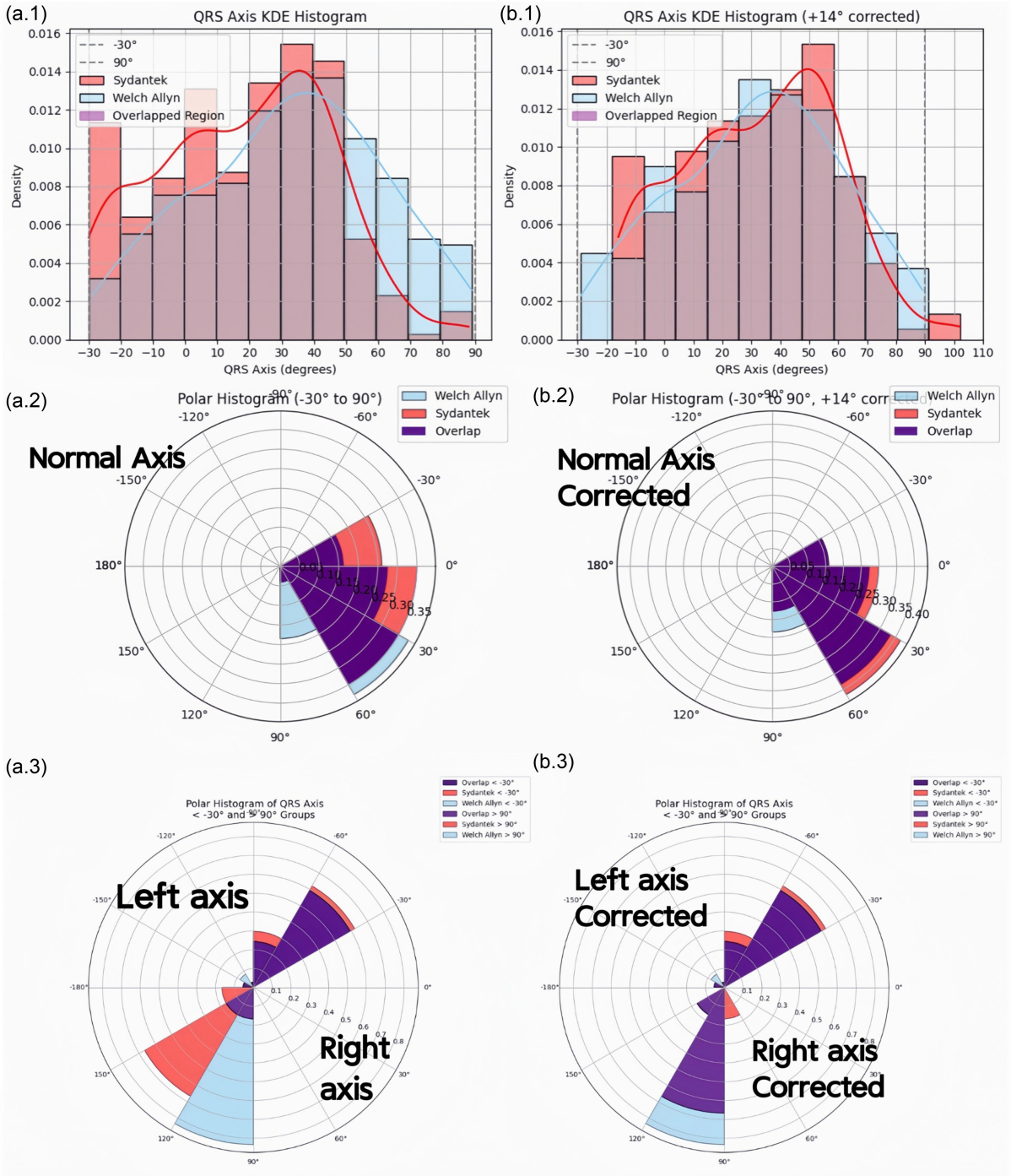

5.4. Implications for workflow and device certification

Given that axis deviation alone seldom drives clinical decisions [2, 17], Sydäntek's stable quadrant behavior and preserved morphology support its use in high-throughput settings—from emergency triage to decentralized care. Its untethered form enables remote ECG monitoring without compromising fidelity—a key advance in diagnostic cardiology [5, 10, 18].

Sydäntek avoids algorithmic axis correction, adhering to a transparent declaration policy. This supports traceability and aligns with ISO/IEC 80601-2-86 standards [8]. In light of rising firmware recalls across wearable devices [19], geometric reproducibility becomes a safety imperative.

Figure 4
Post-correction concordance of ECG vector alignment across coronary territories: spatial shifts requiring clinical reorientation

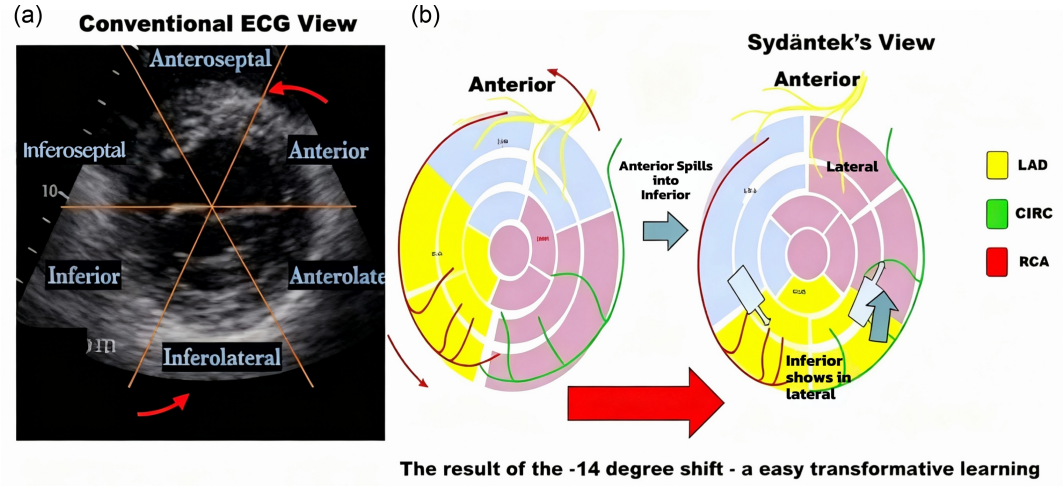

Table 1
In Sydäntek compressed geometry, leads act like windows at a new angle. Anterior activity may project into limb leads like III and aVF, while lateral signals dominate both chest and patch electrodes. For posterior evaluation, clinicians can temporarily reposition V1 to the V3 location—labeling it clearly—to recapture the high-value retrocardiac signal

Analysis of QRS Axis Data and Lead Placement Impact			
Coronary Territory	Conventional Lead View	SydänTek Projection	Interpretive Tip
Inferior (RCA)	II, III, aVF	Inferior signals may shift into V5–V6; some anterior vector crossover into III, aVF	Be alert for "anteriorized" inferior events; contextualize with reciprocal changes
Lateral (Circumflex)	I, aVL, V5–V6	Enhanced via compressed limb patch and lateral precordials	Leads V5–V6 remain reliable indicators; augmented by limb patch projection
Anterior (LAD)	V1–V4	Stable in precordials; signal may spill subtly into III and aVF	Cross-check ST or T-wave changes in III/aVF when anterior pathology suspected
Right Ventricular	V1–V2 (± V3R)	Unchanged; stable over upper sternum	Consistent morphology; wearable design does not compromise early RV signals
Septal	V1–V2	Preserved; slightly broadened anterior coverage	Q waves and R/S ratios remain interpretable; minimal relearning required
Posterolateral	V7–V9 (not routinely used)	Posterior coverage enhanced by repositioning V1 to V3 location	For suspected posterior events, label the repositioned lead as +V1–V3 and interpret accordingly

5.5. Conclusion

Sydäntek—a reimagined wearable ECG platform—achieves diagnostic equivalence with standard systems through a correctable ~14° axis shift. Maintaining waveform fidelity and quadrant placement enables accurate interpretation despite lead redesign. This transformation is consistent, reproducible, and non-disruptive, confirming the feasibility of wearable ECG in clinical practice.

These results contribute to the evolving paradigm of wearable validation. Digital twin models [2, 5], cohort mapping [6, 8], and emerging regulatory frameworks increasingly emphasize signal transformation literacy [14, 20, 21]. Sydäntek exemplifies this shift: a platform grounded in physiological design, informed geometry, and interpretive transparency.

Figure 4: This schematic supports intuitive learning and validates Sydäntek's orientation protocol by aligning conventional labels with physiologically meaningful vector distribution. It demonstrates the sectoral correspondence between regional myocardial labeling in echocardiographic imaging and polar mapping techniques. Figure 4(a) displays a standard ultrasound segmentation of the left ventricle with directional labeling (anteroseptal to inferolateral), serving as a spatial reference. Figure 4(b) compares coronary perfusion territories using two mapping approaches: Conventional Echo View in polar mapping, followed by Sydäntek View. Both formats depict LAD, circumflex, and right coronary artery dominance with color-coded sectors. The Sydäntek View incorporates the counter clockwise -14° rotation and consequences that need enhanced anatomical alignment.

The ~14° axis offset introduced by the Sydäntek wearable geometry does not compromise diagnostic fidelity but does require clinicians to recalibrate spatial expectations. Please note the summary of relearning in Table 1. Interpretation remains intuitive—once the geometric shift is understood, quadrant alignment and waveform morphology remain consistent.

5.5.1. Take-home message

Sydäntek is not merely a miniaturized ECG—it's a geometrically intelligent redesign that compresses Einthoven's triangle without compromising clinical meaning. Its ∼14° axis offset is not an error but a declared artifact of physiological lead repositioning. Understanding this shift empowers clinicians to confidently interpret wearable ECGs, embracing mobility and continuity of care—without relearning the heart, only adjusting the lens.

Ethical Statement

The study follows the Helsinki protocol and the following CTRI/2021/04/032733, Sydantek ECG Equivalence Study trial. The authors declare that all potential respondents were fully informed about the survey and participation was voluntary.

Conflicts of Interest

The authors declare that they have no conflicts of interest to this work.

Data Availability Statement

Data are available from the corresponding author upon reasonable request.

Author Contribution Statement

Sugandhi Gopal: Conceptualization, Methodology, Resources, Data curation, Writing – original draft, Writing – review & editing, Visualization, Supervision, Project administration. **Prabhavathi Bhat:** Validation. **Sharada Sivaram:** Validation. **V J Karthikeyan:** Validation. **Mukund Prabhu:** Validation. **Mohith Subramanian:** Methodology, Software, Formal analysis, Investigation, Data curation, Writing – review & editing, Visualization. **Vishwateja Reddy:** Software, Formal analysis, Investigation. **Aishwarya Srinivasan:** Software, Formal analysis, Investigation.

References

[1] Kayyali, M., Mincholé, A., Qian, S., Young, A., Ugurlu, D., Fairweather, E., . . . , & Lamata, P. (2025). Anatomical-electrical coupling of cardiac axes: Definitions and population variability for advancing personalised ECG interpretation. *PLOS Computational Biology*, *21*(7), e1013161. https://doi.org/10.1371/journal.pcbi.1013161

[2] Corral-Acero, J., Margara, F., Marciniak, M., Rodero, C., Loncaric, F., Feng, Y., . . . , & Lamata, P. (2020). The 'Digital Twin' to enable the vision of precision cardiology. *European Heart Journal*, *41*(48), 4556–4564. https://doi.org/10.1093/eurheartj/ehaa159

[3] Mincholé, A., Zacur, E., Ariga, R., Grau, V., & Rodriguez, B. (2019). MRI-based computational torso/biventricular multiscale models to investigate the impact of anatomical variability on the ECG QRS complex. *Frontiers in Physiology*, *10*, 1103. https://doi.org/10.3389/fphys.2019.01103

[4] Gemmell, P. M., Gillette, K., Balaban, G., Rajani, R., Vigmond, E. J., Plank, G., & Bishop, M. J. (2020). A computational investigation into rate-dependant vectorcardiogram changes due to specific fibrosis patterns in non-ischæmic dilated cardiomyopathy. *Computers in Biology and Medicine*, *123*, 103895. https://doi.org/10.1016/j.compbiomed.2020.103895

[5] Qian, S., Ugurlu, D., Fairweather, E., Toso, L. D., Deng, Y., Strocchi, M., . . . , & Niederer, S. (2025). Developing cardiac digital twin populations powered by machine learning provides electrophysiological insights in conduction and repolarization. *Nature Cardiovascular Research*, *4*(5), 624–636. https://doi.org/10.1038/s44161-025-00650-0

[6] Ugurlu, D., Qian, S., Fairweather, E., Mauger, C., Ruijsink, B., Toso, L. D., . . . , & Bishop, M. (2025). Cardiac digital twins at scale from MRI: Open tools and representative models from ∼ 55000 UK Biobank participants. *PLOS One*, *20*(7), e0327158. https://doi.org/10.1371/journal.pone.0327158

[7] Halvaei, H., Sörnmo, L., & Stridh, M. (2021). Signal quality assessment of a novel ECG electrode for motion artifact reduction. *Sensors*, *21*(16), 5548. https://doi.org/10.3390/s21165548

[8] ISO/IEC 80601-2-86. (2018). *Particular Requirements for the Basic Safety and Essential Performance of Electrocardiographs. Geneva: International Organization for Standardization*, Retrieved from: IEC/AWI 80601-2-86.2 - Medical electrical equipment — Part 2-86: Particular requirements for the basic safety and essential performance of electrocardiographs, including diagnostic equipment, monitoring equipment, ambulatory equipment, electrodes, cables and leadwires

[9] Vukadinovic, M., Kwan, A. C., Yuan, V., Salerno, M., Lee, D. C., Albert, C. M., . . . , & Clarke, S. L. (2023). Deep learning-enabled analysis of medical images identifies cardiac sphericity as an early marker of cardiomyopathy and related outcomes. *Med*, *4*(4), 252–262. https://doi.org/10.1016/j.medj.2023.02.009

[10] Nagar, S. D., Jordan, I. K., & Mariño-Ramírez, L. (2023). The landscape of health disparities in the UK Biobank. *Database*, *2023*, baad026. https://doi.org/10.1093/database/baad026

[11] Ferrer, M. I. (1972). The significance of axis deviation. *Chest*, *61*(1), 2–3. https://doi.org/10.1378/chest.61.1.2

[12] Zhao, X., Zhang, J., Gong, Y., Xu, L., Liu, H., Wei, S., . . . , & Xia, L. (2022). Reliable detection of myocardial ischemia using machine learning based on temporal-spatial characteristics of electrocardiogram and vectorcardiogram. *Frontiers in Physiology*, *13*, 854191. https://doi.org/10.3389/fphys.2022.854191

[13] Man, S., Maan, A. C., Schalij, M. J., & Swenne, C. A. (2015). Vectorcardiographic diagnostic & prognostic information derived from the 12-lead electrocardiogram: Historical review and clinical perspective. *Journal of Electrocardiology*, *48*(4), 463–475. https://doi.org/10.1016/j.jelectrocard.2015.05.002

[14] Ribeiro, A. H., Ribeiro, M. H., Paixão, G. M. M., Oliveira, D. M., Gomes, P. R., Canazart, J. A., . . . , & Ribeiro, A. L. P. (2020). Automatic diagnosis of the 12-lead ECG using a deep neural network. *Nature Communications*, *11*(1), 1760. https://doi.org/10.1038/s41467-020-15432-4

[15] Alipo-on, J. R. T., Escobar, F. I. F., Tan, M. J. T., Karim, H. A., & AlDahoul, N. (2023). ECG-based heartbeat classification using convolutional neural networks. *International Journal of Biomedical and Biological Engineering*, *17*(12), 344–351.

[16] Macfarlane, P.W., Devine, B. & Clark, E. (2005). The University of Glasgow (Uni-G) ECG analysis program. *Computers in Cardiology*, *32*, 451–454. https://doi.org/10.1109/CIC.2005.1588134.

[17] Sia, C., Dalakoti, M., Tan, B. Y. Q., Lee, E. C. Y., Shen, X., Wang, K., Lee, J. S., Arulanandam, S., Chow, W., Yeo, T. J., Yeo, K. K., Chua, T. S. J., Tan, R. S., Lam, C. S. P.,

& Chong, D. T. T. (2019). A Population-wide study of electrocardiographic (Ecg) norms and the effect of demographic and anthropometric factors on selected ECG characteristics in young, Southeast Asian males—Results from the Singapore Armed Forces ECG (Safe) study. *Annals of Noninvasive Electrocardiology*, *24*(3), e12634. https://doi.org/10.1111/anec.12634

[18] Santhanakrishnan, R., Wang, N., Larson, M. G., Magnani, J. W., Vasan, R. S., Wang, T. J., Yap, J., Feng, L., Yap, K. B., Ong, H. Y., Ng, T. P., Richards, A. M., Lam, C. S., & Ho, J. E. (2016). Racial differences in electrocardiographic characteristics and prognostic significance in whites versus Asians. *Journal of the American Heart Association*, *5*(3), e002956. https://doi.org/10.1161/JAHA.115.002956

[19] Hulme GV. (2023). Hardening medical devices' soft and risky security underbelly: firmware [Internet]. NexusConnect; Retrieved from: https://nexusconnect.io/articles/hardening-medical-devices-soft-and-risky-security-underbelly-firmware

[20] Strodthoff, N., Wagner, P., Schaeffter, T., & Samek, W. (2021). Deep Learning for ECG Analysis: Benchmarks and Insights from PTB-XL. *IEEE journal of biomedical and health informatics*, *25*(5), 1519–1528. https://doi.org/10.1109/JBHI.2020.3022989

[21] Singh, A. K., & Krishnan, S. (2023). ECG signal feature extraction trends in methods and applications. *BioMedical Engineering OnLine*, *22*(1), 22. https://doi.org/10.1186/s12938-023-01075-1

How to Cite: Gopal, S., Bhat, P., Sivaram, S., Karthikeyan, V. J., Prabhu, M., Subramanian, M., . . . , & Srinivasan, A. (2025). From Wires to Wearables (1): Clinical equivalence with an Axis-Aware Validation of a Wearable ECG System (Sydäntek) with Compressed Lead Geometry. *Smart Wearable Technology*. https://doi.org/10.47852/bonviewSWT52026869